Response to the Editor's comments

Reviewer 3 suggested changes to the manuscript, that were needed to deal with the question whether or not the data can be used to demonstrate that ozone loss and bromine enhancements were "very fast". The authors initially argued that the changes were happening *in situ,* caused by local chemical processes, and were thus surprisingly fast. However, Reviewer 3 (supported by earlier comments from Reviewer 1) concluded that the reason the changes were fast was because they were driven by transport, something which has been reported previously in the literature. The authors made some requested changes. However, they still present their results on the basis that the rate of change is surprising – if it is transport-driven, the rates of change are not surprising, and should not be over-stated; indeed such changes and rates of change, have been reported in previous papers. Therefore amendments to the manuscript are still needed in a number of places, to adjust the tone of their paper to reflect this fact.

Author's Response:

We are very grateful for the reviewer and editor's valuable comments. Please kindly find the author's responses below.

There are two ways to address the major concerns raised. One would be the following:
i) Remove the sentence (**page 1 line 18 to 20**) that states: "the ozone loss rate during the bromine enhancement period was 10.3 ppbv h^{-1}, which is extremely high compared to those observed in other areas"

Author's Response: The abstract has been revised accordingly.

ii) On **page 2, line 32**, please change the statement " a unique process event" and replace with "an event"

Author's Response: Revised.

iii) **Page 8 line 4 and 5**, change the sentence: "The concurrent changes in the chemical and meteorological variables demonstrate the impact of environment change on this ozone depletion/BrO event" and replace with "The concurrent changes in the chemical and meteorological variables demonstrate that changes in observed chemistry are evident because of changes in transport, albeit on a small scale".

Author's Response: Revised.

iv) **Page 8 line 17 to 19**, please remove the first three sentences of this section; the section should therefore start "The deposition of gaseous mercury…."

Author's Response: Part 4.3 has been revised accordingly.

v) **Page 8 line 23**, remove the statement "The mercury loss rate is ~25 $ngm^{-3}h^{-1}$ or 6 $ngm^{-3}d^{-1}$

Author's Response: Removed.

vi) In the conclusions section**, Page 9 lines 2 to 7,** please remove all the text from "The concurrent changes in chemical and meteorological variables…….Further observations are required to identify its chemical mechanisms"

Author's Response: Removed.

vii) **Page 9 line2**, alter the text to read: "By analysing the air mass history and sea ice conditions, this BrO enhancement event was found to more likely be a regional process, driven by changes in sea ice and transport on a local scale."

Author's Response: Revised.

viii) **Table 2** should also be removed.

Author's Response: Done.

The alternative is that the authors ensure that every time they refer to the rate of changes calculated, they clearly state that these are most likely driven by transport, and then compare the calculated rates of change to those observed by others, and published in the literature. The context is extremely important.

I note also the Author's reply to the minor comment vii), regarding aerosol as surfaces for heterogenous reactions. The authors are correct, that sea salt aerosol has been shown to be an important source of bromine compounds to the atmosphere. However, they confuse the range of different surfaces which can act as a source. For example, in general, salty condensed phases can be a source of bromine compounds, and this can be achieved directly, and not only via producing aerosol. For example, there is evidence now that frost flowers are not a source of aerosol, however they could still be a modest source of bromine compounds directly to the atmosphere. To address this the authors should remove mention of aerosol on **page 2 lines 6 and 8**. On **page 6 line 25**, they should change wording to read: "…frost flowers, which can provide highly concentrated saline surfaces, and also sea salt aerosol." They should also remove the label "aerosol" in **Fig 1**. My view is that the discussion of bromine sources would then be consistent.

Author's Response: We agree with you and have revised the relevant parts following your suggestions.

Observations and ~~the~~ source investigations of the boundary layer BrO in the Ny-Ålesund Arctic

Yuhan Luo[1], Fuqi Si[1], Haijin Zhou[1], Ke Dou[1], Yi Liu[2] and Wenqing Liu[1]

[1] Key Laboratory of Environmental Optics and Technology, Anhui Institute of Optics and Fine Mechanics, ~~Key Laboratory of Environmental Optics and Technology,~~ Chinese Academy of Sciences, Hefei, 230031, China

[2]National Synchrotron Radiation Laboratory, University of Science and Technology of China, Hefei, 230027, China

Correspondence to: Yuhan Luo (yhluo@aiofm.ac.cn) and Fuqi Si (sifuqi@aiofm.ac.cn)

Abstract. During polar spring, the ~~presents~~presence of reactive bromine in the polar boundary layer ~~are~~is considered ~~as~~to be the main cause of ~~the~~ ozone depletion and mercury deposition. ~~But~~However, many uncertainties still remain in understanding the mechanisms of the chemical process and ~~the~~ source of the bromine. As the Arctic sea ice has ~~dramatically~~ recently been dramatically reduced ~~recently~~, it is critical to investigate the mechanisms using more accurate measurements with higher temporal and spatial resolution. In this study, a typical process of enhanced bromine and depleted ozone ~~in late April, 2015~~ in the Ny-Ålesund boundary layer in late April 2015 was observed by applying ground-based ~~Multi~~ Multi-Axis-Differential Optical Absorption Spectroscopy (MAX-DOAS) technique. The results showed that there were BrO slant columns as high as 5.6×10^{14} ~~molecular cm^{-2}~~molec.cm^{-2} ~~BrO slant columns~~ above the Kings Bay area ~~in~~ on 26 April. Meanwhile, the boundary layer ozone and gaseous elemental mercury (GEM) w~~as~~ere synchronously reduced by 85% and 90%, respectively. ~~Considering~~ Based on the meteorology, sea ice distribution and air mass history, the sea ice in the Kings Bay area, which emerged ~~only~~ for only a very short period of time when the enhanced BrO was observed, was considered ~~as~~ to be the major source of this bromine enhancement event. ~~The kinetic calculation showed that the ozone loss rate during the bromine enhancement period is was 10.3 ppbv h^{-1}, which is extremely high compared to those observed in other areas. The GEM loss rate is was approximately about 0.25 ng m^{-3} h^{-1}.~~ The oxidized GEM may be directly deposited onto snow/ice and thereby influence the polar ecosystem.

1 Introduction

Bromine monoxide is one of the key reactive halogen species ~~which have~~that has profound impacts on the ~~atmosphere~~ atmospheric chemistry of the polar boundary layer (PBL), especially the oxidative capacity of the troposphere (Saiz-Lopez and von Glasow, 2012). The presence of reactive bromine (in some situations called "bromine explosion") is considered ~~as~~to be the main cause of the depletion of boundary layer ozone, called "ozone depletion events" (ODEs) (Platt and Hönninger, 2003). Furthermore, halogens can efficiently oxidize gas-phase mercury, which can lead to a decrease of gaseous mercury, called "atmospheric mercury depletion events (AMDEs)" (Ariya et al., 2002; Ariya et al., 2004; Lindberg et al., 2002; Lu et al., 2001; Steffen et al., 2008). Enhanced BrO was first~~ly~~ detected by Long Path Differential Optical Absorption Spectroscopy (LP-DOAS) observations (Platt, 1994). Satellite measurements confirmed that the phenomenon of bromine enhancement covers larger areas of polar regions by deriving daily global BrO maps (Richter et al., 1998); (Platt and Wagner, 1998; Wagner et al., 2001; Sihler et al., 2013). The primary source of reactive bromine has been explained by a series of photochemical and heterogeneous reactions at the surface of~~occurred over the~~ the frozen ocean during polar spring (Fan and Jacob, 1992). A typical heterogeneous reaction model between the gaseous and condensed phases ~~was~~ is shown in Fig. 1. Bromine is released from ~~salty~~ ice surfaces to the atmosphere in an autocatalytic chemical mechanism that oxidizes bromide to reactive bromine. The reaction of HOBr~~ in aerosol~~ is proposed to be the catalyst that drives ~~pivot to explain~~ the recycling reaction, which is an acid-catalyzed reaction (Simpson et al., 2007). Sea-ice (first year) surfaces, brine, and frost flowers have been considered as possible sources~~ of bromide aerosols~~ (Kaleschke et al., 2004) (Lehrer et al., 2004).

However, the ~~true~~actual situation~~ circumstance~~ is that the ODEs do not always occur concurrently~~and~~ with episodes of BrO enhancement~~ are not always in consistency~~. There are only few reports of Arctic ODEs that are assumed to have been observed primarily as a result of local-scale chemical mechanisms (Bottenheim et al., 2009; Jacobi et al., 2006). As the photochemical reactions ~~are quickly~~ happen~~ed~~ quickly and the lifetimes of the intermediate products~~,~~ (e.g. the reactive bromine radicals) are quite short, more accurate data with a higher temporal resolution are needed to analyz~~inge~~ the chemical process in the PBL and investigat~~inge~~

the source of bromine.

The MAX-DOAS (Multi-AXis Differential Optical Absorption Spectrometer) technique has the advantage of being able to clearly separate ~~clearly~~ the tropospheric and stratospheric portions of the atmospheric column~~,~~ and even derive a crude vertical profile (Frieß et al., 2011). When pointing to a direction slightly above the horizon, the spectrometer can obtain high sensitivities for the trace gases close to the ground ~~can be obtained~~ due to the long light path through the trace gas layers. ~~It~~This technique is also an important calibration of satellite observations, which ha~~s~~ve lower spatial and temporal resolutions compared with ground-based measurements. In the Arctic area, ground-based MAX-DOAS observations have been made at Barrow, Alaska (71 °N, 157 °W), Alert, northern Canada (82.5 °N, 62.3 °W) and Ny-Ålesund, Svalbard (78.9° N, 11.8° E) (Tab.1). ~~Besides~~Additionally, air-borne (Neuman et al., 2010; Pöhler et al., 2013) and ship-borne measurements (Bottenheim et al., 2009; Jacobi et al., 2006; Leser et al., 2003; Wagner et al., 2007) are important supplements for the analysis and mode~~l~~ling of bromine chemistry.

However, recently, ~~the~~ Arctic sea ice coverage has dramatically reduced, especially at East Greenland and ~~N~~north of Europe. Influenced by the North Atlantic Warm Current (NAWC), the near-~~-~~surface air temperatures and sea-~~-~~surface temperatures (SST) are ~~getting~~becoming higher ~~at~~in ~~North~~northern Europe (Fig. 2). In recent years, Kings Bay in Ny-Ålesund has ice-free open water all year round, which is a unique characteristic ~~comparing~~ compared with other parts at the same latitude in the Arctic. Therefore, it is critical to have a better understanding of the possible sources of the reactive bromine ~~source~~ and the impact of ~~the~~ halogen activation on PBL ozone depletion and mercury deposition ~~under~~ within a rapidly changeing Arctic.

In this study, ~~we have~~ caught an ~~unique process~~ event of enhanced bromine and depleted ozone in Ny-Ålesund was caught in late April. The key role of bromine was confirmed by ground-based MAX-DOAS measurements. This event provides a rare opportunity to investigate the source of bromine and the process of ozone depletion at this area. ~~Kinetic studies of ozone depletion and gaseous mercury deposition are discussed afterwards.~~

2 Instruments and methods

2.1 Instrument setup

The MAX-DOAS measurement site is located at Yellow River Station (78°55′30″ N, 11°55′20″ E) at Ny-Ålesund~~,~~ on the west coast of Spitsbergen. The observation position is shown in Fig. 3. To ~~have~~ give a rough idea of the climate conditions, monthly mean sea ice concentration~~s~~ anomalies and air temperature anomalies ~~in~~ during April 2015 are shown~~demonstrated~~ in Fig. 2. ~~The observations~~ Observations were ~~carried out~~obtained from 25 April to 15 May 2015. Due to the wavelength adjustment, no data ~~is~~ were available during a short period from 28 to 29 April.

The MAX-DOAS instrument operated at Ny-Ålesund consists of both indoor and outdoor parts. The telescope ~~receiving~~ receives scattered sunlight from multiple angles ~~is~~ and is controlled by a stepper motor to adjust elevation angles from horizon (0°) to zenith (90°). The field of view of the telescope is approximately~~about~~ 1°. The scattered sun light is imported through the quartz fiber with a numerical aperture of 0.22 into the indoor spectrograph (Ocean Optics MAYA pro) with a ~~one~~ one-dimensional CCD array (ILX511 linear array CCD) containing 2068 pixels. The wavelength range of the spectrograph is from 290 nm to 420 nm, thus enabling the analysis of trace gases including O_3, NO_2, BrO, OClO, HCHO, and O_4. The spectral resolution is ~~about~~ approximately 0.5 nm (FWHM). The CCD detector is cooled at -30 ℃, while the whole spectrometer is thermally stabilized at +20 ℃ using a thermal controller. A computer sets the configuration of the system and controls the automatic measurements. The integration time (typically ranging from 100 ms to 2000 ms in multiple of 100 scans~~ times~~) of each measurement depends on the intensity of scattered light, which can be influenced by clouds and visibility. ~~The~~ A standard mercury lamp is used for spectra calibration. Calibration measurements of dark current and offset are performed after each measurement.

The telescope is pointed towards the n~~N~~ortheast direction, which covers the Kings Bay area (Fig. 3). Kings Bay is an inlet on the west coast of Spitsbergen, one part of the Svalbard archipelago in the Arctic Ocean. The inlet is 26 km long and 6 to 14 km wide. The range of MAX-DOAS measurement is an area with a radius of approximately~~about~~ 10 km ~~radius area~~, which covers the central area of the fjord. The sequence of elevation angles is 2°, 3°, 4°~~, 5°~~, 6°, 8°, 10°, 15°, 30° and 90° above the horizon.

2.2 Data evaluation

The spectra, measured with the setup ~~above~~ described above, ~~setup~~ are analyzed using the well-established DOAS retrieving method (Platt, 1994). The wavelength calibration ~~was~~ is performed using the QDOAS software developed by the Belgian Institute for Space Aeronomy (BIRA) by fitting the reference spectrum to a ~~high~~ high-resolution Fraunhofer spectrum (Kurucz et al., 1988). The spectral analysis of BrO is performed at 340-359 nm, encompassing three BrO absorption~~s~~ bands, which improves the accuracy of the inversion. O_3 (223K, 243K) (Bogumil et al., 2003; Vandaele et al., 1998), NO_2 (298K, 220K) (Vandaele et al., 1998), O_4 (Hermans et al., 2003), BrO (228K) (Wilmouth et al., 1999), OClO (233K) (Kromminga et al., 2003), and Ring Structure (Chance and Spurr, 1997) are involved in the inversion algorithm. The O_4 retrieval is performed using the same set of cross sections as for BrO but in the wavelength interval ~~at~~ of 340-370 nm. The ~~high~~ high-resolution cross sections ~~were~~ are convoluted with the instrument slit function determined by measuring the emission line of a mercury lamp. A ~~fifth~~ fifth-order ~~of~~ polynomial ~~was~~ is applied to eliminate the broad band structures in the spectra caused by Rayleigh and Mie scattering. Furthermore, a nonlinear intensity offset ~~was~~ is included in the fit to account for possible instrumental stray light. A wavelength shift and stretch of the spectra ~~was~~ are allowed in the fit in order to compensate for small changes in the spectral adjustment of the spectrograph.

The fit procedure yields differential slant column densities (~~dSCD~~DSCD) using ~~noon time~~ zenith sky measurements of each sequence as Fraunhofer reference for the analysis, which eliminates the influence of stratospheric BrO change. An example of the fit result of BrO ~~and O_4~~ is shown in Fig. 4. The spectrum was recorded on 26 April~~,~~ 2015 19:59 UTC (SZA=86 °) at the elevation angle of 2 °. The BrO ~~dSCD~~ DSCD is 5.10×10^{14} ~~molecular cm^{-2}~~ molec.cm^{-2}. The residual root mean square is 4.59×10^{-4}, resulting in a statistical BrO ~~dSCD~~ DSCD error of 1.63×10^{13} ~~molecular cm^{-2}~~ molec.cm^{-2}. ~~The DSCDs of BrO at elevation angle 2 °were obtained by subtracting 90 °of each sequence, which eliminate the influence of stratosphere BrO change.~~

Since DSCDs are dependent on the light path, wavelength and observation geometry, DSCDs are then converted to vertical column density (VCD) by dividing by the differential air mass factor (DAMF), which is the averaged light path enhancement for solar light traveling through the atmosphere compared to a straight vertical path.

We perform the radiative transfer modeling (RTM) simulations using SCIATRAN software (Rozanov et al., 2005) to ~~get~~obtain the modeled DAMF using five different assumed BrO profiles with evenly distributed air masses: a. 0-0.5 km; b. 0-1 km; c. 0-2 km; d. 0.5-1 km; e. 1-2 km (Fig. 5a). The models are performed under clear sky conditions with no aerosol input. Remarkable differences exist~~s~~ for different input profiles. For the BrO layers of 0-0.5 km, 0-1 km and 0-2 km, the DAMFs all increase with ~~the~~ decrease~~e~~ing ~~of~~ elevation angles. ~~While~~However, for the BrO layers of 0.5-1 km and 1-2 km, the dependence on the telescope elevation angle is weaker, especially at small elevation angles.

The modeled BrO DSCDs for different input BrO profiles are shown in Fig. 5b. The input BrO VCD is 5×10^{13} molecules/cm^2. The measured BrO DSCDs from 26 April 20:00 (UTC) ~~26/04~~ to 27 April 0~~5~~4:00 (UTC) ~~27/04~~ are also plotted (Fig. 5c). ~~The blue dots indicate data points for the first 4 hours in 26/04, while red and orange dots indicate later 4 hours in the morning of 27/04~~. Since the inaccuracy of modeled BrO becomes larger at lower elevation angles, elevation angles of $\geq 8°$ should receive more attention. From Fig. 5b, we can obviously see that the measured BrO DSCDs are best reproduced by the model for layer 0-1 km before midnight. This suggests that the BrO layer between 0-1 km can be considered as the most likely~~possible~~ distribution ~~of BrO layer, which is compatible with the measurements~~. Thereby, BrO ~~SCDs can be converted to~~ volume mixing ratios (VMR) are calculated assuming a homogeneous BrO layer with a thickness of 1 km ~~thickness~~ at the surface.

2.3 Complementary data

Ny-Ålesund is a science community hosting over fifteen permanent research stations. Atmospheric measurements have been measured continuously at Zeppelin Station, Ny-Ålesund since 1990. Located on Zeppelin Mountain, with an altitude of 474 meters a.s.l., it is a background atmosphere observatory operated by ~~NPI (~~ the Norwegian Polar Institute (NPI) and ~~NILU (~~the Norwegian Institute for Air Research (NILU) , which are part of the Global Atmosphere Watch (GAW) Framework.

At the Zeppelin Station, ~~S~~surface ozone was measured by UV photometry, ~~–~~ and ~~G~~gaseous mercury in the air was measured using a Tekran mercury detector. Hourly ~~Surface~~ surface ~~Ozone~~

ozone and gaseous mercury data are downloaded fromat the EBAS database (Tørseth et al., 2012). Meteorology data, including temperature, air pressure, relative humidity, wind direction and velocity, and global radiation data are recorded by the AWIPEV Atmospheric Observatory in Ny-Ålesund. According to the radiosondes records of temperature, humidity and wind speed from AWIPEV, the height of the troposphere is aroundapproximately 8000 meters and the height of the boundary layer is aroundapproximately 1200 meters at Ny-Ålesund.

A Wwebcam on the 474 m Zeppelin Mountain records the sea ice change of Kings Bay and the cloud situation of Ny-Ålesund. (https://data.npolar.no/_file/zeppelin/camera/)

In order to get a To roughly estimate the idea of BrO distribution, BrO maps of the northern hemisphere by GOME-2 products are downloaded from http://www.iup.uni-bremen.de/doas/scia_data_browser.htm. Stations overpass BrO vertical column densities for MetOp-A (GOME-2A) and MetOp-B (GOME-2B) in the Ny-Ålesund, Arctic are downloaded from https://avdc.gsfc.nasa.gov/index.php?site=580525926&id=97.

Using the Hybrid Single-Particle Lagrangian Integrated Trajectory (HYSPLIT) model via the NASA ARL READY website (http://www.ready.noaa.gov/ready/open/hysplit4.html) (Draxler and Rolph, 2013; Stein et al., 2015), back trajectory analyses were carried out to find determine the history of air masses. 72-hours ensemble back Back trajectories of 72 hours were driven by meteorological fields from the NCEP Global Data Assimilation System (GDAS) model output.

3 Results

The Ttime series of BrO DSCDs at 2 °, surface ozone concentrations, solar zenith angle (SZA), air pressure, air temperature, relative humidity, wind velocity and wind direction from 25 April to 15 May are presented in Fig. 6. Starting from late afternoon in 26 April, BrO DSCDs clearly exceeded the background levels and peaked at 5.6×10^{14} molecular cm^{-2}molec.cm^{-2}. At In the same period, surface ozone sharply decreased from ~80 ppb to several ppb and did not recovered to normal values until 29 April. During this period, the wind velocity is more thanchanged frequently between 1-7 5 m/s, with unstable wind directions and mixing heightsand decreases in 29 April. Over a period of one week, elevated BrO levels went back down to the detection limit byin 4 May under a stable boundary layer. During 4-5 May, partial ozone (not to near the zero level) was

depleted in the absence of BrO.

The ~~T~~time series of BrO ~~d~~DSCDs from 26 April 14:00 (UTC) ~~26 April~~ to 28 April 12:00 (UTC) ~~28 April in~~ at every elevation angle (2 °, 3 °, 4 °, 6 °, 8 °, 10 °, 15 °, 30 °) are plotted in Fig. 7. Results of different elevation angles were ~~distinguished~~ obviously distributed during the BrO enhancement period. However, ~~But~~ the differences ~~of~~in the BrO ~~d~~DSCDs $\leqslant 4°$ are very small (upright plot in Fig. 7), indicating that the highest value of BrO is probably not above the surface. ~~In order t~~To ~~have a~~ better understand~~ing of~~ the vertical distribution of reactive bromine at the Arctic boundary layer, a comparison between the measured BrO DSCDs from the MAX-DOAS measurements with the modeled ones from the SCIATRAN model ~~are~~ is performed (Fig. 5). The measured BrO DSCDs best match the model for the 0-1 km layer during the enhancement, which means that the BrO enhancement event was a regional rather than an in situ process. ~~BrO layer height between 0-1 km is considered as the most possible distribution of BrO layer, which is compatible with the measurementBrO dSCDs distributed from 0-1 km to more likely at 0.5-1 km along with time. This could be explained by that Br/BrO photochemistry reactions are taking place from the boundary layer to the free troposphere where there is enough ozone to react.~~

The ~~S~~sunshine duration, ~~global radiation,~~ SZA, BrO DSCDs from the MAX-DOAS at a 2 ° elevation angle, BrO volume mixing ratio, surface ozone and gaseous mercury data from 26-28 April are plotted in Fig. 8. The BrO VMRs were calculated assuming a 0-1 km layer of the BrO profile. The highest BrO VMR is approximately~~about~~ 15 pptv during the ODE. Ozone, as well as gaseous mercury, dropped extremely fast right after the enhancement of BrO. ~~But~~However, there seems to be ~~not~~ insufficient reactive bromine present~~ed~~ locally in the boundary layer since the ozone ~~turned to~~ slowly increases just four hours later (at 26 April 2~~3~~1:00 UTC ~~26 April~~). Afterwards, both ozone and mercury have a slow~~ly~~ recovery with a fluctuation ~~in~~on ~~the~~ 27 April ~~afternoon~~. A tiny increase of BrO occurs around 27 April 20:00 (UTC). This could be explained by the fact that Br/BrO photochemistry reactions are taking places where there is enough ozone to react. When ozone drops to the lower limit of the reaction, the reaction of $Br+O_3 \rightarrow BrO+O_2$ would stop (i.e., the situation observed on the night of 26 April). When ozone recovers to a certain level, the reaction starts again.

4 Discussions

In this research, high concentrations of tropospherice BrO has have been detected using the ground-based MAX-DOAS technique. A BrO column asAs high as 5.6×10^{14} molecular cm^{-2}molec.cm^{-2} BrO column has beenwas detected above Kings Bay, Ny-Ålesund. The retrieval shows that the enhancement occurred accompanied with by severe ozone depletion and mercury deposition.

The Ppossible sources of the reactive bromine are newly formed sea ice and frost flowers, which can provide highly concentrated saline surfaces, and also sea salt aerosolthereby, adequate sea saltbromine aerosols. The transport of the air masses that which already contain elevated BrO or precursors and depleted ozone, is another possible source of enhanced BrO. Therefore, we investigated the history of the air masses arriving at the measurement site using backward trajectories. Furthermore, the sea ice distribution (Fig.2) and the satellite BrO maps (Fig. 10) also provide are important informationinstructions as well.

This enhancement event is represented a good opportunity to investigate the source of the BrO and the its impact on the environment of the Arctic boundary layer. These issues are discussed in detail in theThe following sections based on theparts are discussed in detail from air mass history, sea ice distribution, and ozone loss and mercury deposition data.

4.1 History of air masses

Possible sources of reactive bromine are newly formed sea ice and frost flowers which can provide highly concentrated saline surfaces, thereby adequate sea salt aerosols. Another important source is the transport of the air masses which already contain elevated BrO and depleted ozone. Therefore, we investigate the history of the air masses arriving at measurement site using backward trajectories. Furthermore, the sea ice distribution (Fig.2) and the satellite BrO maps (Fig.10) are important instructions as well.

To find the details of the air mass origin, 72-hour backward trajectories at altitudes ofNy-Ålesund (10 and, 500, 1000 meters a.s.l.) from 26 April (0600 UTC) toending at 27 April 18:00 (UTC) 27

April (1800 UTC) were calculated every 6 hours (Fig. 9a). This calculation shows that air masses at both altitudes have a discontinuous origin. Then, we calculated the air mass backward trajectory ending at 26 April 18:00 (UTC) for every hour (Fig. 9b). This calculation shows that the air mass has different origin before/after 26 April 15:00 (UTC). The wind direction changed to the north direction with higher velocity. After, the air mass had a relatively stable origin from a height of 1000 m. From the map of three altitudes, air masses turned from northwest direction, which is origin from North America to the middle of Arctic Sea. From the vertical distribution of air masses, before noon of 26 April, the air masses came from low boundary layer, while after 18:00 26 April, from the upper troposphere.More trajectory calculations from 22 April to 30 April are shown in Appendix Fig. A1 and Fig. A2 for purposes of comparisons.

From the GOME-2 BrO VCD maps from 24 April to 27 April (Fig. 10), we found that enhanced BrO was observed at the east of Greenland (red box), far north of Siberia (blue circle) and east of Spitsbergen (black box) during the period of interest and the days before. The BrO maps from other days (20 April to 13 May 2015) are shown in Appendix Fig. A3.

GOME-2 BrO VCD maps from GOME-2 measurements from 20 April to 13 May 2015 are shown in Fig. 10. BrO clouds existed at two main periods: coastal North America and Chukchi Sea during 22-23 April and North of Siberia during 08-11 May 2015. Both of the BrO clouds lasted about three to four days, the first of which was occasionally at the same period with the Ny-Ålesund BrO enhancement event. Combining the GOME-2 BrO maps and the trajectory calculations, the role of long range transport source of air masses can be discussed in detail. Firstly, trajectory calculations showed that transport from the east coast of Greenland and east coast of Spitsbergen is not possible. SoThus, transport from these areas of enhanced BrO can very probablymost likely be ruled out. Second, trajectories also showed that after 26 April 16:00 (UTC), transport from the north occurred, which means the high BrO in the blue circle might have influenced this event. However, a) the altitude of the air mass is reaches up to 1000 m; b) there is no enhancement along the path; and c) the time scale is unreasonable. The BrO enhancement we found by the ground-based MAX-DOAS, as well as ozone loss, only lasted for several hours. However, the high level of BrO in the blue circle area lasted for more than one day. Secondly, transport from the north takes place. However, rather low BrO VCDs is showed directly north of Spitsbergen. during the period of interest and the days before, enhanced BrO VCDs are observed

~~northeast of Spitsbergen~~

~~However, what we found by ground-based MAX-DOAS just lasted for several hours, which is at different time scale. Thereby, air masses transported from high latitude of Arctic from 22 April might have an impact on BrO enhancement in Ny-Ålesund, but not the most critical reason.~~

Additionally, the transport of air masses ~~might~~may be the reason that the~~of the slowly back~~ BrO concentrations were slow to return to normal values until 3 May.

4.2 Sea ice distribution

~~According to t~~The observations of sea ice concentration from the AMSR-E and Zeppelin webcam~~,~~ indicated that Kings Bay ~~is~~ was an ice-free water area during the measurement period. However, large amounts of sea ice appeared at Kings Bay on 26 April (Fig. 11), floating from the bay entrance by both wind and tidal forces, which is an unusual phenomenon in the fjord.~~and lasted for few hours~~ . The shape of sea ice ~~was~~comprised broken ice pieces with irregular borders. ~~The i~~Ice ~~sea~~ water mixture ~~was~~ filled in the gaps between sea ice~~, which was salty-enriched~~. From the shape of the ice in Fig. 11, the sea ice did not look like newly formed sea ice because of its irregular pieces and corrugated edges. Therefore, we consider that the sea ice was formed before floating in the bay and transformed into the ice-water mixture when it came across sharply dropped temperatures.

The chemical and meteorological information from the start of 26 April to noon on 28 April are shown together in Fig. 12. When ozone depletion/BrO enhancement occurs, the air temperature continuously decreases, and the relative humidity drops from 80% to less than 65%, with the wind direction switching from northwest to east. The concurrent changes in the chemical and meteorological variables demonstrate that changes in observed chemistry are evident because of changes in transport, albeit on a small scale.~~the impact of environment change on this ozone depletion/BrO enhancement event.~~

~~The efficient ozone loss is consistent with the temperature decline (Fig.12). The meteorology data shows that on 26 April air temperature continually goes down and reaches bottom of -11.4°C at 22:00. According to the precipitation curve of calcium carbonate, more than 80% of carbonate precipitates below 265K. This process will provide acid aerosol from alkaline sea water, which~~

~~triggers the transformation of inert sea-salt bromide to reactive bromine (Sander et al., 2006). Although the sun radiation intensity is not strong at that time, the heterogeneous reactions can still happen under the twilight.~~ It is also worth noting that the time periods when the sea ice existed and the time BrO started to become enhanced (and the ozone was depleted) were not exactly the same. Fig. 8 and Fig. 12 indicated that the ozone loss started from 26 April 14:00 (UTC). As described above, the sea ice existed in the fjord after 26 April 20:00 (UTC). This observation makes the synchronizing variations in BrO and ozone, as well as the 0-1 km distribution, reasonable.

~~Thereby~~Therefore, this BrO enhancement event is more likely a regional~~local~~ process~~,~~ mainly influenced by ~~underlying surface change and~~ the local environment. The sea ice is not totally fresh ice, but the low air and water temperatures during this period may have caused the formation of the brine ice mixture, which is the source of the bromine radicals. The surface ozone concentrations increased along with the melting of sea ice, which indicated that the life spans of the BrO radicals are very short. ~~When sea ice disappeared, the~~ The ~~reaction immediately ended and~~ reactive bromine radicals gradually transformed to soluble bromide (e.g., HOBr), which explained the sink of ~~it~~ bromine (Fan and Jacob, 1992).

4.3 ~~Kinetic analysis~~M~~Ozone depletion and m~~ercury deposition

~~What makes this case study uniquevery special is that the increasing rate of BrO and the depletion rate of boundary layer ozone are really both very fast. The surface ozone was reduced by 85% within 4 hours. The ozone loss rate is was as high as 10.3 ppbv h^{-1} or 248 ppbv d^{-1}, which is extremely high compared with previous studies in Polar Regions (Tab. 2).~~ The deposition of gaseous mercury occurred concurrently with tropospheric ozone depletion, as well as the enhancement of BrO (Fig. 1~~4~~3), which indicat~~ed~~es that the oxidation of GEM by reactive halogen species (Br atoms and BrO radicals) is considered to be the key process of mercury depletion. The GEM decreases from ~2 ng m^{-3} to lower than 0.3 ng m^{-3} during the BrO enhancement event. The oxidized GEM may be directly deposited onto snow/ice or associated with particles in the air that can subsequently be deposited onto ~~the~~ snow and ice surfaces~~,~~ and thereby threatens polar ecosystems and human health.

The chemical kinetics of bromine enhancement and ozone decay are analyzed assuming that the catalytic reactions are dominated by reactions showed in Fig.1. A first-order loss of ozone is due to reaction $Br+O_3 \rightarrow BrO+O_2$ resulting in the rate law:

$$r = -\frac{d[O_3]}{dt} = k_1 \cdot [O_3] \quad \text{(Eq. 1)}$$

$$[O_3] = [O_3]_0 \cdot \exp(-k_1 \cdot t) \quad \text{(Eq. 2)}$$

$$\ln\frac{[O_3]}{[O_3]_0} = -k_1 \cdot t \quad \text{(Eq. 3)}$$

$[O_3]_0$ is the ozone concentration at the beginning of decay determined from the measured mixing ratio of 74.72 ppbv. $\ln\frac{[O_3]}{[O_3]_0}$ versus time are showed as hollow square in Fig. 13a.

According to the method by Jacobi et al. (Jacobi et al., 2006), the first order rate constant k_1 can be determined as follows:

$$\frac{d(\ln\frac{[O_3]}{[O_3]_0})}{dt} = -k_1 \quad \text{(Eq. 4)}$$

The measured decrease of $\ln\frac{[O_3]}{[O_3]_0}$ versus time was fitted by:

$$-\ln\frac{[O_3]}{[O_3]_0} = -\exp(b \cdot t + a) \quad \text{(Eq. 5)}$$

$$\frac{d(\ln\frac{[O_3]}{[O_3]_0})}{dt} = -b \cdot \exp(b \cdot t + a) \quad \text{(Eq. 6)}$$

$$-\ln(-\ln\frac{[O_3]}{[O_3]_0}) = b \cdot t + a \quad \text{(Eq. 7)}$$

$$k_1 = b \cdot \exp(b \cdot t + a) \quad \text{(Eq. 8)}$$

$\ln(-\ln\frac{[O_3]}{[O_3]_0})$ versus time are plotted as black dots in Fig. 13a. The coefficients a and b are obtained from the linear fit in plot.

The ozone loss begins relatively slow and accelerates with time, which is consistent with the

~~process of bromine explosion.~~

~~Assuming that the first order decay is dominated by the reaction $Br+O_3 \rightarrow BrO+O_2$, we are able to calculate the Br concentrations as follows:~~

$$k_1 = k_{Br} \cdot [Br] \quad \text{(Eq. 9)}$$

$$k_{Br} = 1.7 \cdot 10^{-11} \cdot \exp\left(-\frac{800}{T}\right) \quad \text{(Eq. 10)}$$

~~k_{Br} is a constant depending on temperature (Fig. 13b). Thereby, the calculated Br concentration increases from 1.1×10^7 to about 1.2×10^9 atoms cm^{-3} (corresponding to 44.8 pptv) (Fig. 13c). Considering the assumption that the halogens are homogenously distributed in the PBL, the concentrations of Br at sea surface layer in the bromine explosion could be even higher.~~

5 Conclusions

The ~~T~~typical process of enhanced bromine and depleted ozone in the Ny-Ålesund boundary layer was observed using ground-~~-~~based MAX-DOAS techniques in late April~~,~~ 2015. BrO DSCDs a~~A~~s high as 5.6×10^{14} ~~molecular cm^{-2}~~ molec.cm^{-2} ~~BrO DSCDs~~ were detected on 26-27 April. Meanwhile, severe ozone depletion and mercury deposition occurred under a BrO VMR of 15 pptv. The model showed enhanced BrO distributed at 0-1 km above the sea surface. By analyzing the air mass history and sea ice conditions, this BrO enhancement event was found to~~is~~ more likely be a ~~local~~ regional process, driven by changes in sea ice and transport on a local scale. ~~The concurrent changes in chemical and meteorological variables demonstrate the impact of environment change on this ozone depletion/BrO enhancement event. The underlying sea ice and low temperature provide acid aerosols, which are prerequisites for the formation of BrO radicals. The kinetic analysis shows that the ozone loss begins relatively slow and accelerates with time, which is consistent with the process of bromine explosion. The ozone loss rate is as high as 10.3 ppbv h^{-1}, which is much higher than those observed in previous studies in Polar Regions. The GEM loss rate is about ~0.25 ng m^{-3} h^{-1}. This study is represents a pivotal complement for BrO research in Arctic BL. Further observations and analysis are required to identify the its chemical mechanisms.~~

Acknowledgements.

We appreciate the valuable comments from three anonymous referees. This research was financially supported by the National Natural Science Foundation of China (Project No. 41676184, 41306199 and U1407135). We gratefully thank the Chinese Antarctic and Arctic Administration and the teammates of the 2015 Chinese Arctic Expedition. We are also grateful to Dr. Ping Wang from KNMI and Dr. Yang Wang from MPIC for providing the advice ~~on~~ about the BrO VMR calculation. We kindly acknowledge the AWIPEV Atmospheric Observatory in Ny-Ålesund, the Norwegian Polar Institute (NPI) and the Norwegian Institute for Air Research (NILU) for the complementary data. Caroline Fayt, Thomas Danckaert and Michel van Roozendael from BIRA are gratefully acknowledged for providing the QDOAS analysis software. Meteorological ~~data~~, surface ozone, and gaseous mercury data ~~were~~ are provided by the EBAS database. ~~Back trajectories were calculated using the HYSPLIT model from NOAA together with the GDAS data set from NCEP. The authors~~We gratefully acknowledge the NOAA Air Resources Laboratory (ARL) for ~~the provision~~providing ~~of~~ the HYSPLIT transport model and READY website (http://www.ready.noaa.gov) used in this publication.

References

Ariya, P. A., Alexei Khalizov, A., and Gidas, A.: Reactions of gaseous mercury with atomic and molecular halogens: Kinetics, product studies, and atmospheric implications, Journal of Physical Chemistry A, 106, 7310-7320, 2002.

Ariya, P. A., Dastoor, A. P., Marc, A., Schroeder, W. H., Leonard, B., Kurt, A., Farhad, R., Andrew, R., Didier, D., and Janick, L.: The arctic: A sink for mercury, Tellus, 56, 397-403, 2004.

Bogumil, K., Orphal, J., Homann, T., Voigt, S., Spietz, P., Fleischmann, O. C., Vogel, A., Hartmann, M., Kromminga, H., and Bovensmann, H.: Measurements of molecular absorption spectra with the sciamachy pre-flight model: Instrument characterization and reference data for atmospheric remote-sensing in the 230~~–2~~380 nm region, Journal of Photochemistry & Photobiology A Chemistry, 157, 167-184, 2003.

Bottenheim, J. W., Netcheva, S., Morin, S., and Nghiem, S. V.: Ozone in the boundary layer air over the arctic ocean: Measurements during the tara transpolar drift 2006-2008, Atmospheric Chemistry & Physics, 9, 4545-4557, 2009.

Chance, K. V., and Spurr, R. J. D.: Ring effect studies: Rayleigh scattering, including molecular parameters for rotational ~~raman~~ Raman scattering, and the ~~f~~Fraunhofer spectrum, Applied Optics, 36, 5224-5230, 1997.

Hysplit (hybrid single-particle lagrangian integrated trajectory) model access via ~~noaa~~ NOAA ARL~~arl~~ READY ~~ready~~, 2013.

Fan, S. M., and Jacob, D. J.: Surface ozone depletion in arctic spring sustained by bromine reactions on aerosols, Nature, 359, 522-524, 1992.

Frieß, U., Hollwedel, J., König-Langlo, G., Wagner, T., and Platt, U.: Dynamics and chemistry of tropospheric bromine explosion events in the ~~antarctic~~ Antarctic coastal region, Comptes Rendus Des Séances De La Société De Biologie Et De Ses Filiales, 109, 1454-1456, 2004.

Frieß, U., Sihler, H., Sander, R., Pöhler, D., Yilmaz, S., and Platt, U.: The vertical distribution of bro and aerosols in the arctic: Measurements by active and passive differential optical absorption spectroscopy, Journal of Geophysical Research Atmospheres, 116, 597-616, 2011.

Hönninger, G., and Platt, U.: Observations of ~~bro~~ BrO and its vertical distribution during surface ozone depletion at ~~alert~~Alert, Atmospheric Environment, 36, 2481-2489, 2002.

Hebestreit, K., Stutz, J., Rosen, D., Matveiv, V. V., Peleg, M., Luria, M., and Platt, U.: ~~Doas~~ DOAS measurements of tropospheric bromine oxide in mid-latitudes, Science, 283, 55-57, 1999.

Hermans, C., Vandaele, A. C., Fally, S., Carleer, M., Colin, R., Coquart, B., Jenouvrier, A., and Merienne, M. F.: Absorption cross-section of the collision-induced bands of oxygen from the ~~uv~~ UV to the ~~nir~~NIR, Springer Netherlands, 193-202 pp., 2003.

Jacobi, H., Kaleschke, L., Richter, A., Rozanov, A., and Burrows, J. P.: Observation of a fast ozone loss in the marginal ice zone of the Arctic Ocean, Journal of Geophysical Research Atmospheres, 111, 3363-3375, 2006.

Kaleschke, L., Richter, A., Burrows, J., Afe, O., Heygster, G., Notholt, J., Rankin, A. M., Roscoe, H. K., Hollwedel, J., and Wagner, T.: Frost flowers on sea ice as a source of sea salt and their influence on tropospheric halogen chemistry, Geophysical Research Letters, 31, 371-375, 2004.

Kromminga, H., Orphal, J., Spietz, P., Voigt, S., and Burrows, J. P.: New measurements of ~~oclo~~ OClO absorption cross-sections in the 325-435 nm region and their temperature dependence between 213 and 293 k, Journal of Photochemistry & Photobiology A Chemistry, 157, 149-160, 2003.

Kurucz, R. L., Furenlid, I., Brault, J., and Testerman, L.: Solar flux atlas from 296 to 1300 nm,

National Solar Observatory Atlas, Sunspot, New Mexico: National Solar Observatory, 1988.

Lehrer, E., Hönninger, G., and Platt, U.: A one dimensional model study of the mechanism of halogen liberation and vertical transport in the polar troposphere, Atmospheric Chemistry & Physics, 4, 2427-2440, 10.5194/acp-4-2427-2004, 2004.

Leser, H., Hönninger, G., and Platt, U.: MaxDOAS measurements of BrO and NO2 in the marine boundary layer, Geophysical Research Letters, 30, 149-164, 2003.

Lindberg, S. E., Brooks, S., Lin, C. J., Scott, K. J., Landis, M. S., Stevens, R. K., Goodsite, M., and Richter, A.: Dynamic oxidation of gaseous mercury in the ~~arctic~~ Arctic troposphere at polar sunrise, Environmental Science & Technology, 36, 1245-1256, 10.1021/es0111941, 2002.

Lu, J. Y., Schroeder, W. H., Barrie, L. A., Steffen, A., Welch, H. E., Martin, K., Lockhart, L., Hunt, R. V., Boila, G., and Richter, A.: Magnification of atmospheric mercury deposition to polar regions in springtime: The link to tropospheric ozone depletion chemistry, Geophysical Research Letters, 28, 3219-3222, 2001.

Mcconnell, J. C., Henderson, G. S., Barrie, L., Bottenheim, J., Niki, H., Langford, C. H., and Templeton, E. M. J.: Photochemical bromine production implicated in ~~arctic~~ Arctic boundary-layer ozone depletion, Nature, 355, 150-152, 1992.

Neuman, J. A., Nowak, J. B., Huey, L. G., Burkholder, J. B., Dibb, J. E., Holloway, J. S., Liao, J., Peischl, J., Roberts, J. M., and Ryerson, T. B.: Bromine measurements in ozone depleted air over the ~~arctic~~ Arctic ocean, Atmospheric Chemistry & Physics, 10, 6503-6514, 2010.

Pöhler, D., Stephan, G., Zielcke, J., Shepson, P. B., Sihler, H., Stirm, B. H., Frieß, U., Pratt, K. A., Walsh, S., and Simpson, W. R.: Horizontal and vertical distribution of bromine monoxide in northern ~~alaska~~ Alaska during BROMEX~~bromex~~ derived from airborne imaging-doas measurements, EGU General Assembly Conference, 2013.

Platt, U.: Differential optical absorption spectroscopy (DOAS), in: Air monitoring by spectroscopic techniques, m.W. Sigrist, ed, Chem.anal.ser, 32, 327-333, 1994.

Platt, U., and Wagner, T.: Satellite mapping of enhanced bro concentrations in the troposphere, Nature, 395, 486-490, 1998.

Platt, U., and Hönninger, G.: The role of halogen species in the troposphere, Chemosphere, 52, 325, 2003.

Richter, A., Wittrock, F., Eisinger, M., and Burrows, J. P.: Gome observations of tropospheric bro in

northern hemispheric spring and summer 1997, Geophysical Research Letters, 25, 2683-2686, 1998.

Rozanov, A., Rozanov, V., Buchwitz, M., Kokhanovsky, A., and Burrows, J. P.: Sciatran 2.0 - A new radiative transfer model for geophysical applications in the 175-2400nm spectral region, Advances in Space Research, 36, 1015-1019, 2005.

Saiz-Lopez, A., Mahajan, A. S., Salmon, R. A., Bauguitte, S. J., Jones, A. E., Roscoe, H. K., and Plane, J. M.: Boundary layer halogens in coastal antarctica, Science, 317, 348-351, 2007.

Saiz-Lopez, A., and von Glasow, R.: Reactive halogen chemistry in the troposphere, Chemical Society Reviews, 41, 6448-6472, 10.1039/c2cs35208g, 2012.

Sander, R., Burrows, J., and Kaleschke, L.: Carbonate precipitation in brine ~~–~~ a potential trigger for tropospheric ozone depletion events, Atmospheric Chemistry & Physics, 6, 4653-4658, 2006.

Schroeder, W. H., Anlauf, K. G., Barrie, L. A., Lu, J. Y., Steffen, A., Schneeberger, Amp, D. R., and Berg, T.: Arctic springtime depletion of mercury, Nature, 394, 331-332, 1998.

Sihler, H., Platt, U., Frieß, U., Doerner, S., and Wagner, T.: Satellite observation of the seasonal distribution of tropospheric bromine monoxide in the arctic and its relation to sea-ice, temperature, and meteorology, EGU General Assembly 2013.

Simpson, W. R., Carlson, D., Nninger, G. H., Douglas, T. A., Sturm, M., Perovich, D., and Platt, U.: First-year sea-ice contact predicts bromine monoxide (BrO) levels at barrow, Alaska better than potential frost flower contact, Atmospheric Chemistry & Physics, 6, 11051-11066, 2007a.

Simpson, W. R., Glasow, R. V., Riedel, K., Anderson, P., Ariya, P., Bottenheim, J., Burrows, J., Carpenter, L. J., Frieß, U., and Goodsite, M. E.: Halogens and their role in polar boundary-layer ozone depletion, Atmospheric Chemistry & Physics, 7, 4375-4418, 2007b.

Sinreich, R., Merten, A., Molina, L., and Volkamer, R.: Parameterizing radiative transfer to convert max-doas dscds into near-surface box averaged mixing ratios and vertical profiles, Atmospheric Measurement Techniques, 5, 7641-7673, 2013.

Steffen, A., Douglas, T., Amyot, M., Ariya, P., Aspmo, K., Berg, T., Bottenheim, J., Brooks, S., Cobbett, F., and Dastoor, A.: A synthesis of atmospheric mercury depletion event chemistry in the atmosphere and snow, Atmospheric Chemistry & Physics, 8, 1445-1482, 2008.

Stein, A. F., Draxler, R. R., Rolph, G. D., Stunder, B. J. B., Cohen, M. D., and Ngan, F.: NOAA's HYSPLIT ~~Noaa's hysplit~~ atmospheric transport and dispersion modeling system, Bulletin of the American Meteorological Society, 96, ~~150504130527006~~2059-2077, 2015.

Stutz, J., Thomas, J. L., Hurlock, S. C., Schneider, M., Glasow, R. V., Piot, M., Gorham, K., Burkhart, J. F., Ziemba, L., and Dibb, J. E.: Long-path ~~doas~~ DOAS observations of surface ~~bro~~ BrO at ~~summit~~Summit, ~~greenland~~Greenland, Atmospheric Chemistry & Physics, 11, 9899-9910, 2011.

Tørseth, K., Aas, W., Breivik, K., Fjæraa, A. M., Fiebig, M., Hjellbrekke, A. G., Lund Myhre, C., Solberg, S., and Yttri, K. E.: Introduction to the european monitoring and evaluation programme (~~emep~~EMEP) and observed atmospheric composition change during 1972–2009, Atmos. Chem. Phys., 12, 5447-5481, 10.5194/acp-12-5447-2012, 2012.

Tuckermann, M., Ackermann, R., Gölz, C., Lorenzen-Schmidt, H., Senne, T., Stutz, J., Trost, B., Unold, W., and Platt, U.: Doas observation of halogen radical atalysed arctic boundary layer ozone destruction during the arctoc ampaigns 1995 and 1996 in ny- lesund, spitsbergen, Tellus Series B-chemical & Physical Meteorology, 49, 533-555, 1997.

Vandaele, A. C., Hermans, C., Simon, P. C., Carleer, M., Colins, R., Fally, S., Merienne, M. F., Jenouvrier, A., and Coquart, B.: Measurements of the no2 absorption cross section from 42000cm-1 to 10000cm-1 (238-1000nm) at 220k and 294k, J. ~~quant~~Quant. ~~.spectrosc~~Spectrosc. ~~.radiat~~Radiat. ~~.transfer~~Transfer, 59, 171-184, 1998.

Wagner, T., Leue, C., Wenig, M., Pfeilsticker, K., and Platt, U.: Spatial and temporal distribution of enhanced boundary layer bro concentrations measured by the ~~gome~~ Gome instrument aboard ~~ers~~ERS-2, Journal of Geophysical Research Atmospheres, 106235, 225-224, 2001.

Wagner, T., Ibrahim, O., Sinreich, R., Frie, U., Glasow, R. V., and Platt, U.: Enhanced tropospheric bro over ~~antarctic~~ Antarctic sea ice in mid-winter observed by ~~max~~MAX-DOAS ~~doas~~ on board the research vessel ~~polarstern~~Polarstern, Atmospheric Chemistry & Physics, 7, 3129-3142, 2007.

Wilmouth, D. M., Hanisco, T. F., And, N. M. D., and Anderson, J. G.: Fourier transform ultraviolet spectroscopy of the A $^2\Pi_{3/2} \leftarrow$ X $^2\Pi_{3/2}$ Transition of BrO, ~~a 2e aF., And, N. M. D., and Anderson~~Journal of Physical Chemistry A.~~phys.chem.a~~, 103, 8935-8945, 1999.

Table 1. Comparisons of BrO mixing ratios at four main Arctic observation sites

Sites	Observation periods	BrO mixing ratio	Methods	References
Greenland ice sheet (72N, 38W, 3200 m a.s.l.)	14 May-15 June 2007, 9 June-8 July 2008	3-5 ppt	LP-DOAS	(Stutz et al., 2011)
Barrow, Alaska (71°19'N, 156°40'W)	26 February-16 April 2009	~30 ppt	MAX-DOAS LP-DOAS	(Frieß et al., 2011)
Alert, Nunavut (82°32'N, 62°43'W)	20 April--9 May 2000	~30 ppt	MAX-DOAS	(Hönninger and Platt, 2002)
Ny-Ålesund, Svalbard (78.9N, 11.8E)	20 April-27 April 1996	~30 ppt	LP-DOAS	(Tuckermann et al., 1997)

~~**Table 2. Comparisons of BrO mixing ratios and ozone loss rates**~~

~~**Method**~~	~~**BrO mixing ratio**~~	~~**Typ. Rate of O_3 destruction**~~	~~**References**~~
~~**Observation at PBL**~~	~~up to 30 pptv~~	~~1-2 ppbv h^{-1}~~	~~(Tuckermann et al., 1997; Hönninger and Platt, 2002)~~
~~**Observation at MIZ**~~	~~~63 pptv~~	~~6.7 ppbv h^{-1} or 160 ppbv d^{-1}~~	~~(Jacobi et al., 2006)~~
~~**Observation at salt lakes**~~	~~up to 176 pptv~~	~~10-20 ppbv h^{-1}~~	~~(Hebestreit et al., 1999; Stutz et al., 2011)~~
~~**Observation at Marine BL**~~	~~~2 pptv~~	~~~0.05 ppbv h^{-1}~~	~~(Leser et al., 2003)~~
~~**Model**~~	~~30-40 pptv~~	~~7.6 ppbv d^{-1}~~	~~(Lehrer et al., 2004)~~
~~**Model**~~	~~100 pptv~~	~~40 ppbv d^{-1}~~	~~(Fan and Jacob, 1992)~~
~~**Observation at Ny-Ålesund BL**~~	~~~15 pptv~~	~~10.3 ppbv h^{-1} or 248 ppbv d^{-1}~~	~~**this study**~~

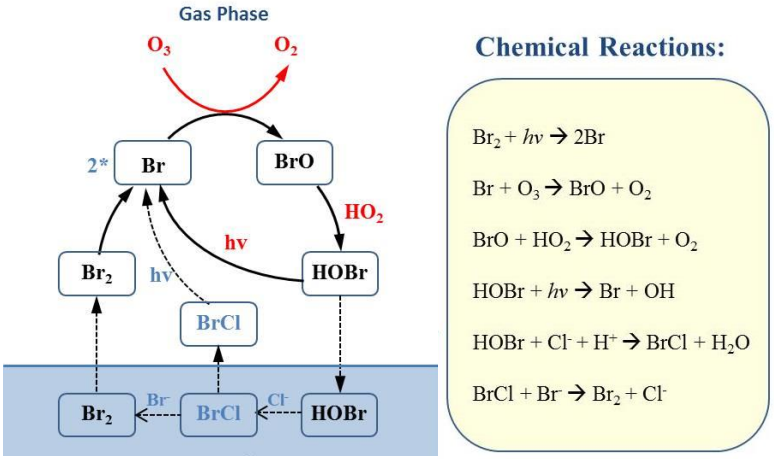

Fig. 1 Chemical reactions of the BrO-~~Ozone~~ ozone cycle

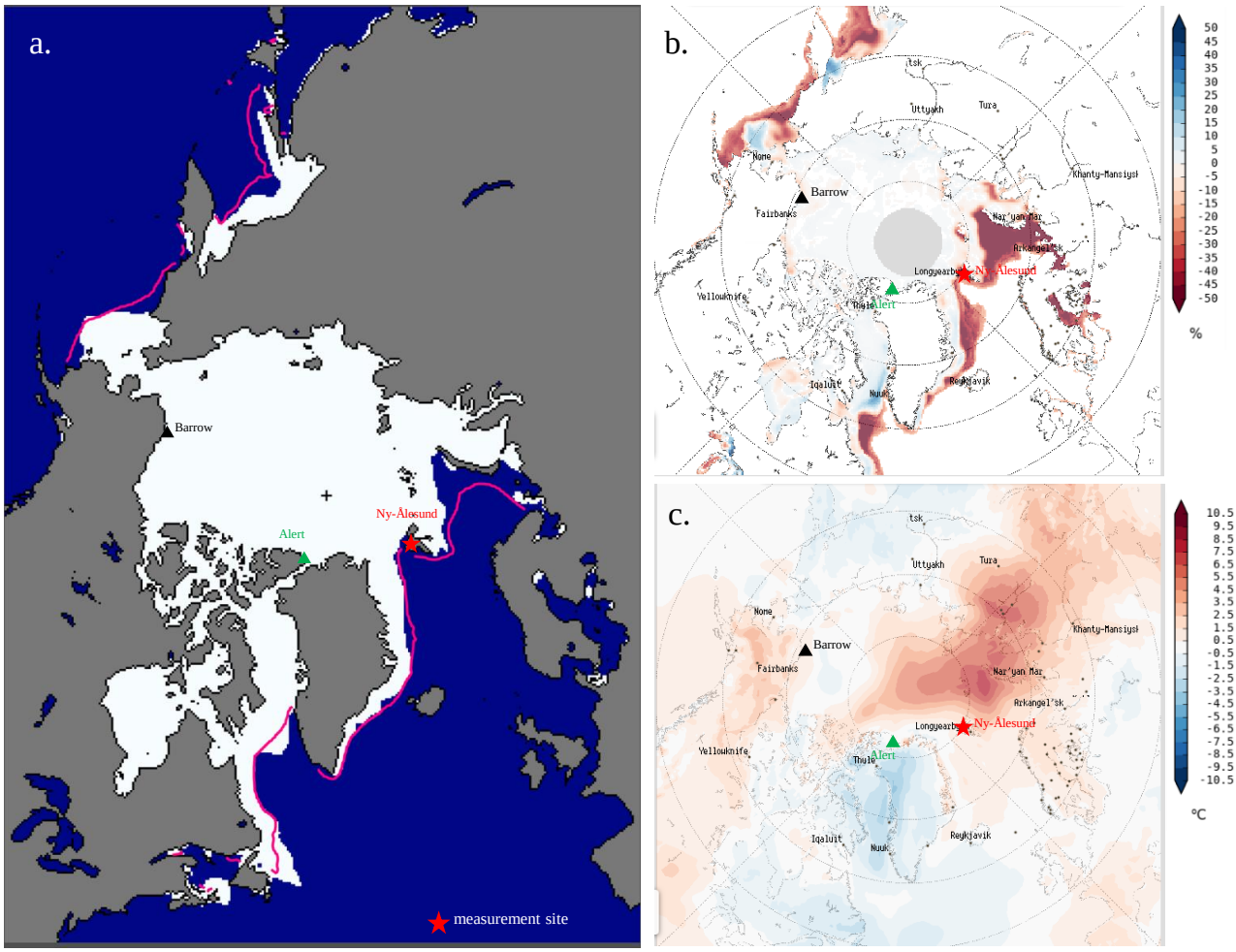

Fig. 2~~.~~ a. Sea ice extent ~~of~~ on April 2015 in the Arctic area (data from http://nsidc.org/data/seaice_index/); b. Monthly mean sea ice concentration~~s~~ anomalies ~~of~~on April 2015 compared to averages from 1979 to 2015~~.~~; c. ~~Two~~2 m~~eters~~ air temperature anomalies ~~of~~ on April 2015 compared to averages from 1979 to 2015 (b and c data are from http://nsidc.org/soac)

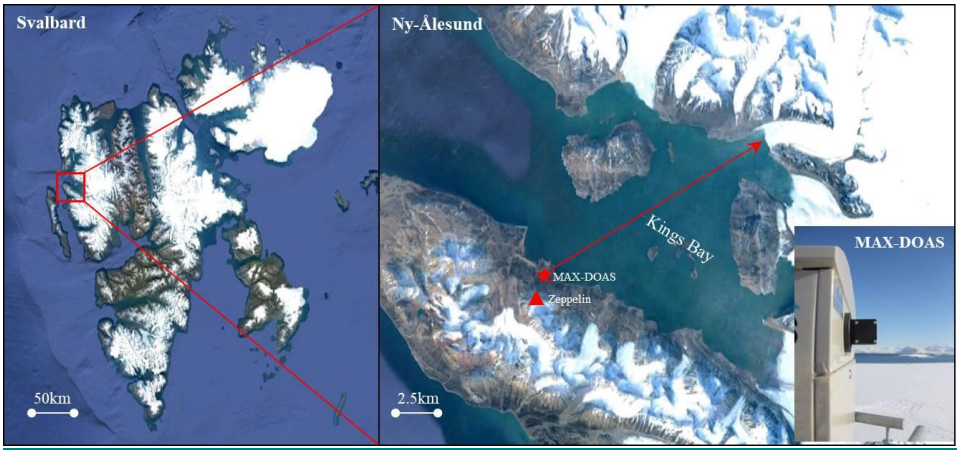

Fig. 3 The MAX-DOAS field observation in Ny-Ålesund, Arctic

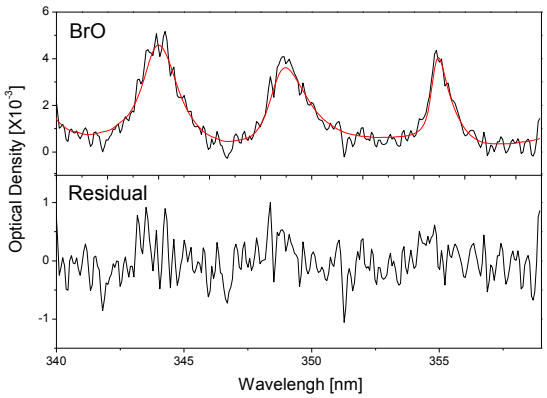

Fig. 4 Examples ofor spectral retrieval of BrO and O4. The spectrum was recorded under clear sky conditions at 2 °elevation on 26 April 2015, 19:59 UTC, SZA = 86 °. (Black lines: Retrieved retrieved spectral signatures fitted result for absorber; red lines: fitted cross sections)

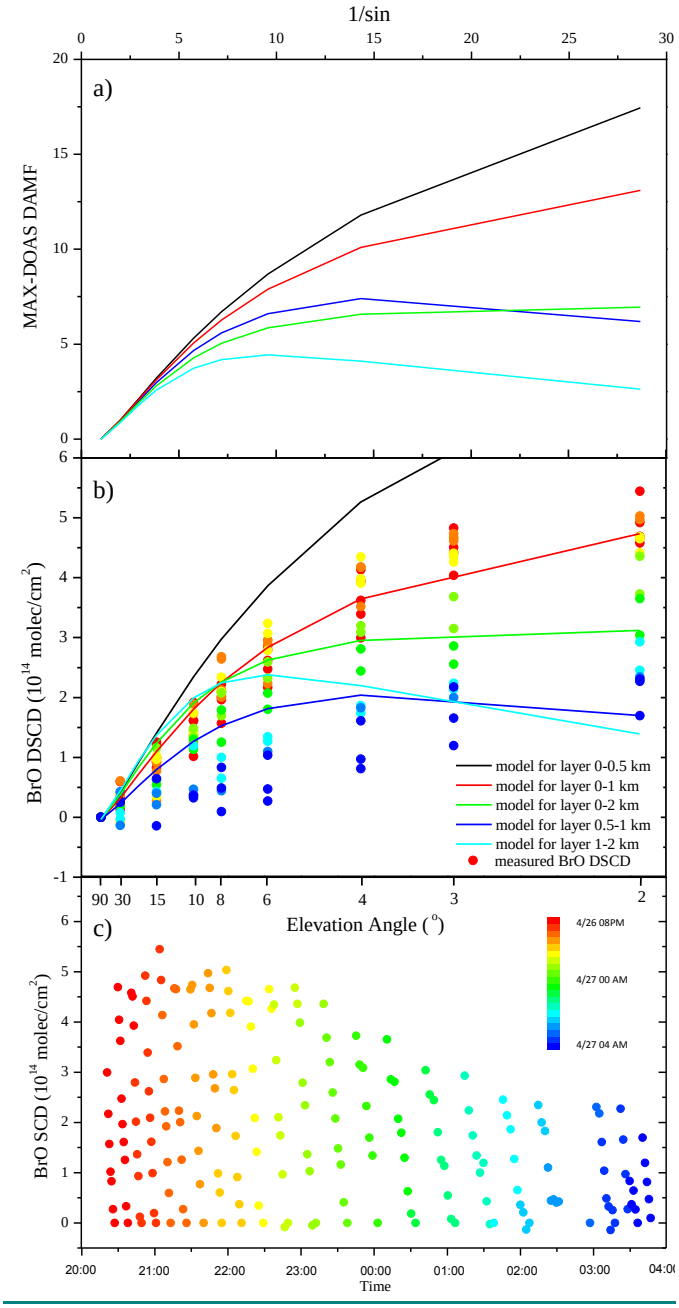

Fig. 5 ~~The m~~Modeled DAMF (a) and BrO ~~slant columns~~DSCD (b) using radiative transfer modeling simulation.

DAMF are the differences of AMF for low elevation angles and zenith direction. The models are performed assuming ~~a~~ clear sky conditions with no aerosol. In part b, the tropospheric BrO VCD is 5×10^{13} molec~~ules/~~.cm^{-2}. The measured BrO DSCDs during the event are also shown (solid dots). The color codes of the measured BrO DSCDs, which are also shown in 5b (solid dots), are put into a one-to-one correspondence with the dots in 5c.

~~The blue dots indicated data points from 20:00 to 24:00 in the evening of 26/04. The red and orange dots indicated data points from 00:00-4:00 in the morning of 27/04.~~

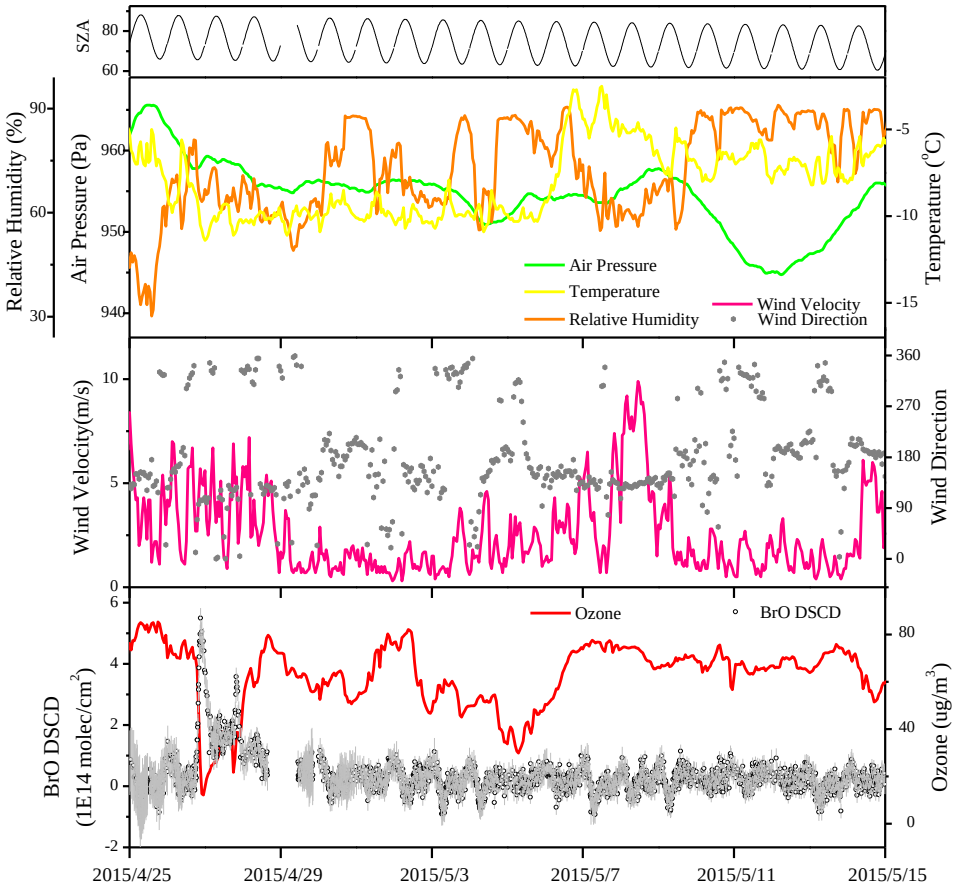

Fig. 6 Time series of BrO ~~dSCDs~~ DSCDs at 2°, surface ozone, SZA and meteorology data during the measurement.

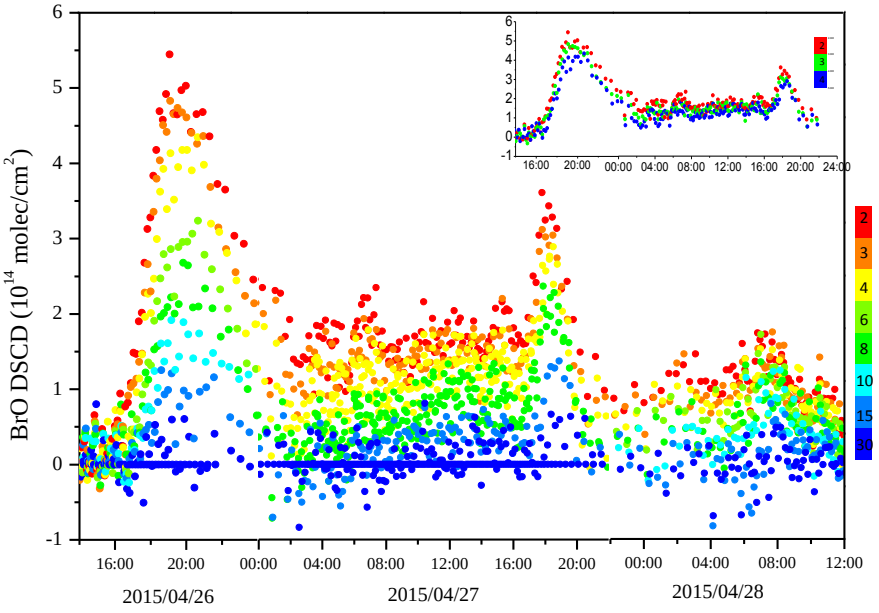

Fig. 7 BrO ~~dSCDs~~ DSCDs of different elevation angles during the enhancement period

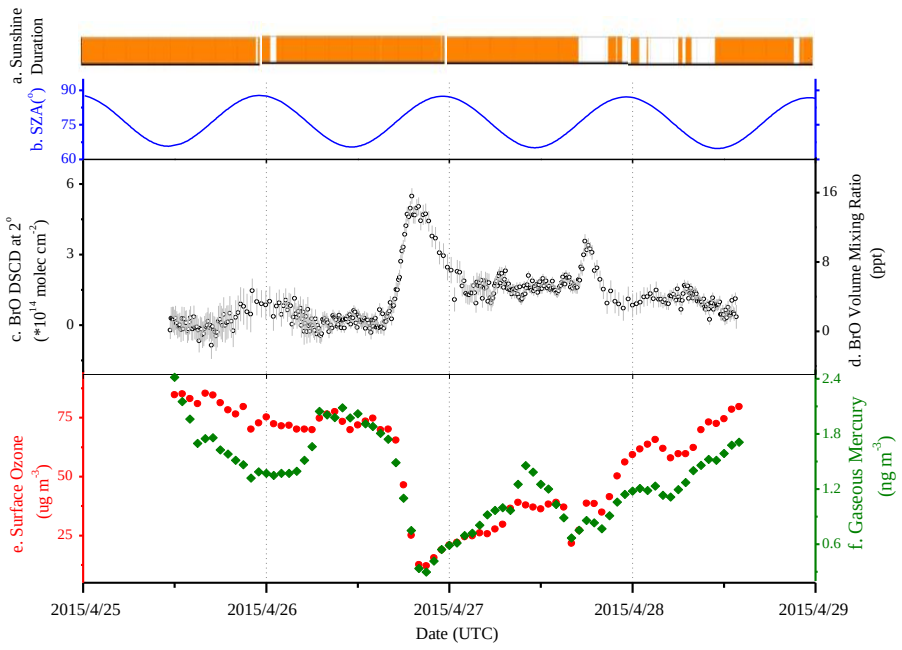

Fig. 8 a. ~~Global radiation (W/m^2) (Cited from AWIPEV database)~~Sunshine duration; b. SZA; c. BrO DSCDs from MAX-DOAS at elevation angle of 2 °; d. BrO VMR (ppt); e. surface ozone (ug/m^3); and f. gaseous mercury (ng/m^3) from 25/04 noon to 28/04 noon 2015. BrO mixing ratios are calculated assuming a homogeneous BrO layer of 0-1 km.

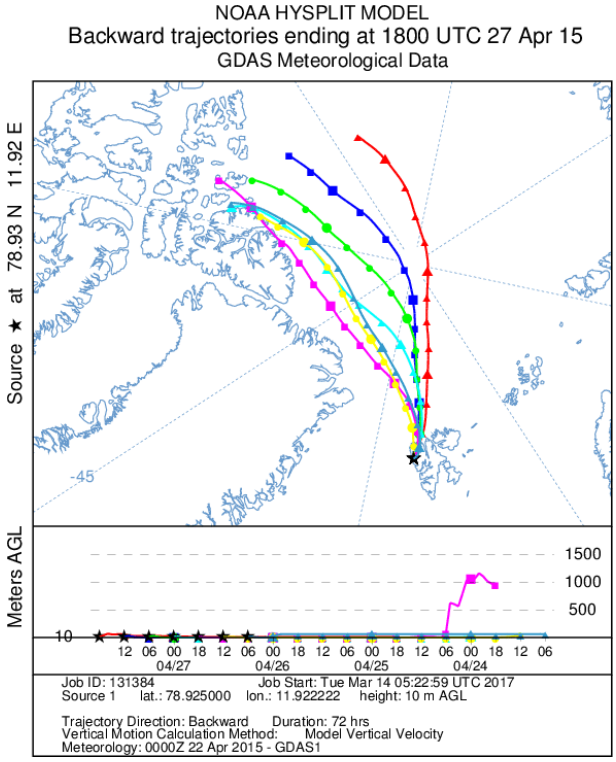

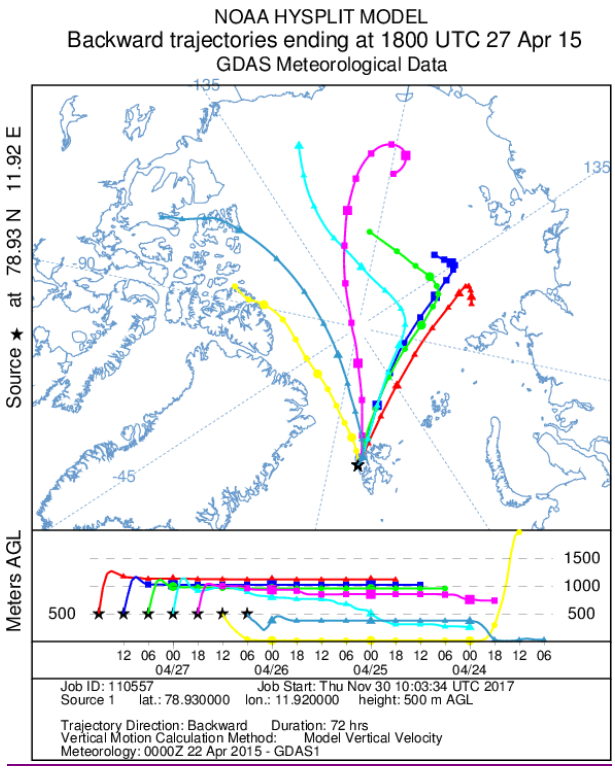

Fig. 9 a. Back trajectory model of air masses arriving at Ny-Ålesund ~~from 26 April (0600 UTC) to~~ending at 27 April ~~(~~18:00 (UTC) at 10~~,~~ and 500~~,~~ ~~1000~~ ~~meters~~ a.s.l.~~.~~ Every 6 h a new trajectory starts, and each trajectory runs for 72 h.

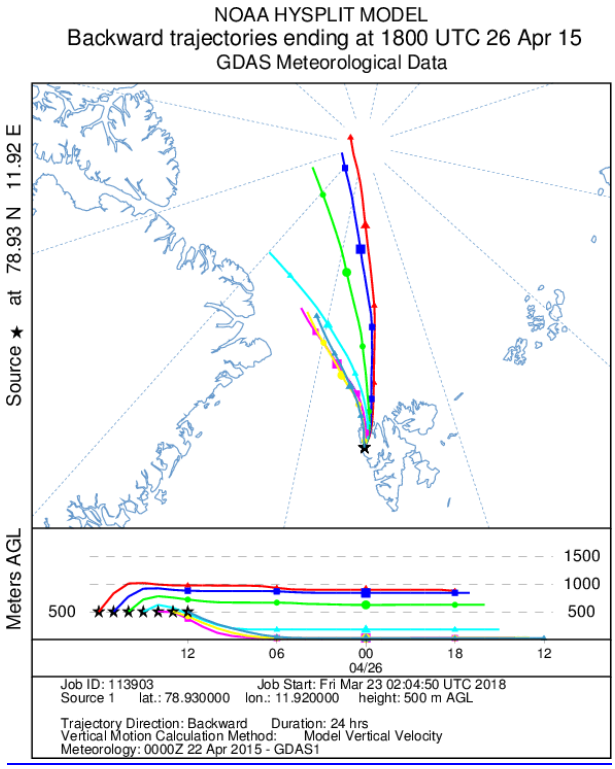

Fig. 9 b. Back trajectory model of air masses arriving at Ny-Ålesund ending at 26 April 18:00 (UTC) at 10 and 500 m a.s.l. Every 6 h a new trajectory starts

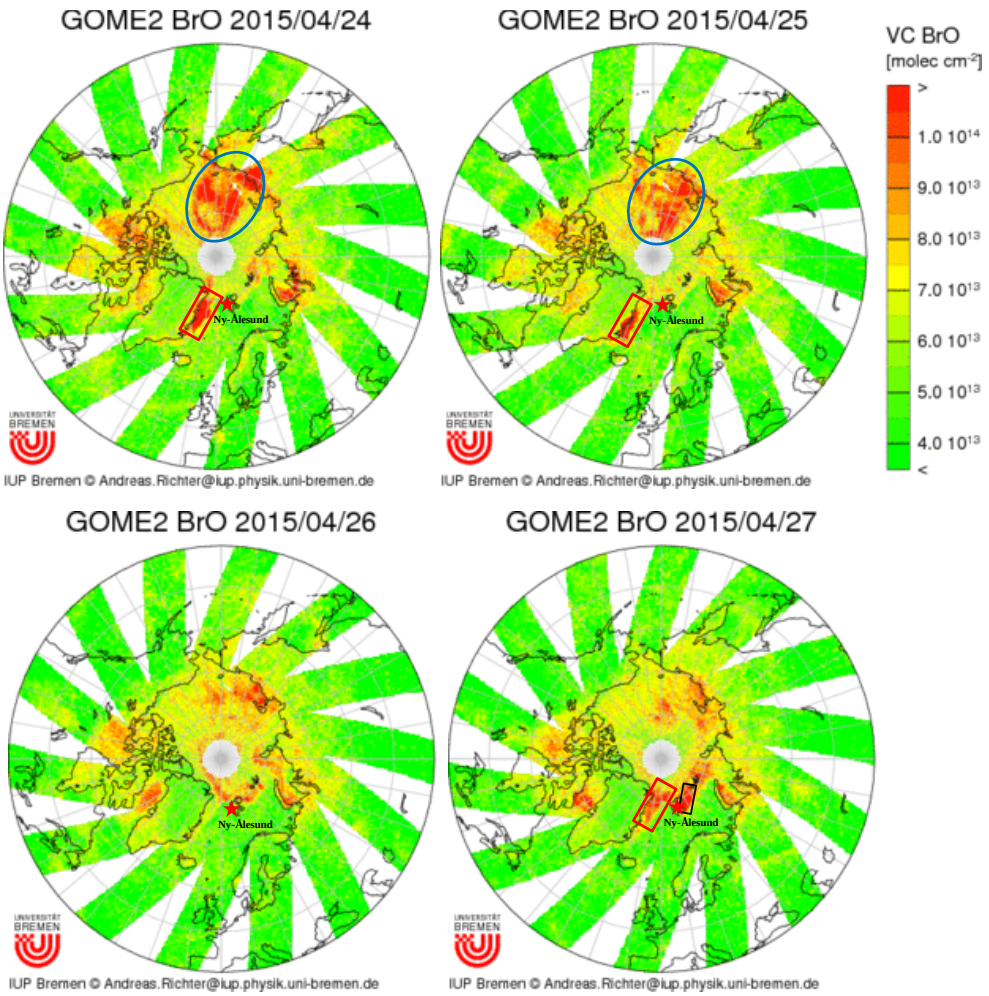

Fig. 10 Map of ~~troposphere~~ tropospheric BrO of the northern hemisphere by GOME-2 products from 2~~0~~4 April to ~~13~~ 27 April~~May~~. (cited from ~~Cited from~~ http://www.iup.uni-bremen.de/doas/scia_data_browser.htm)

Fig. 11 Sea ice in Kings Bay, Ny-Ålesund at ~~22~~26 April 21:00 (UTC), ~~26 April~~ 2015 (at Ny-Ålesund Dock, photograph by Yuhan Luo)

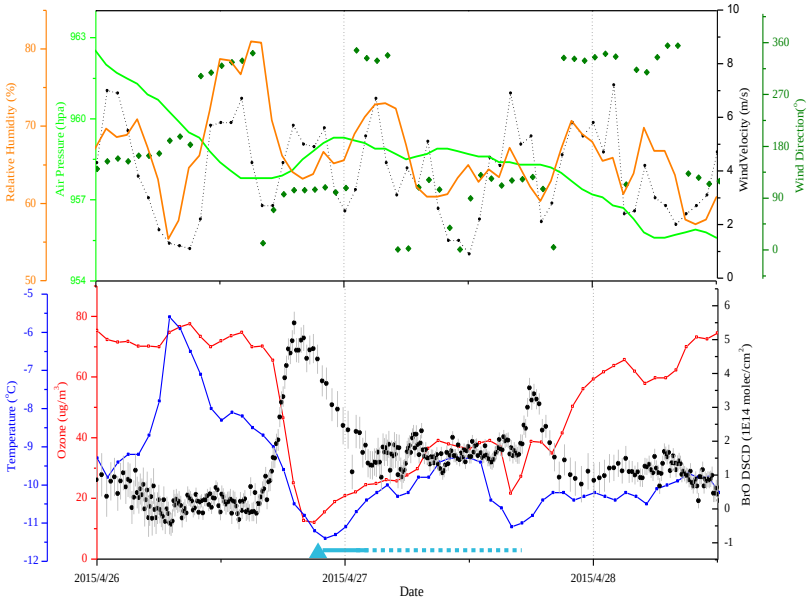

Fig. 12 Time series of chemical and meteorological changes~~surface ozone and air temperature~~ during the BrO enhancement event~~,~~ ; blue triangles represent the existence of sea ice ~~existence~~ in Kings Bay

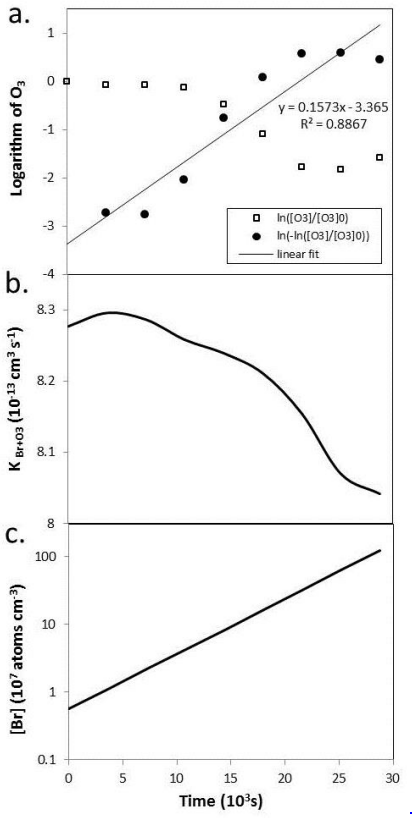

~~Fig.13 Analysis of surface ozone loss in 26 April 2015~~

~~a. Plot of ln([O_3]/[O_{3t0}]) and ln(-ln([O_3]/[O_{3t0}])) versus time; b. Calculated temperature dependent reaction rate coefficients for O_3+Br; c. Calculated Br concentration.~~

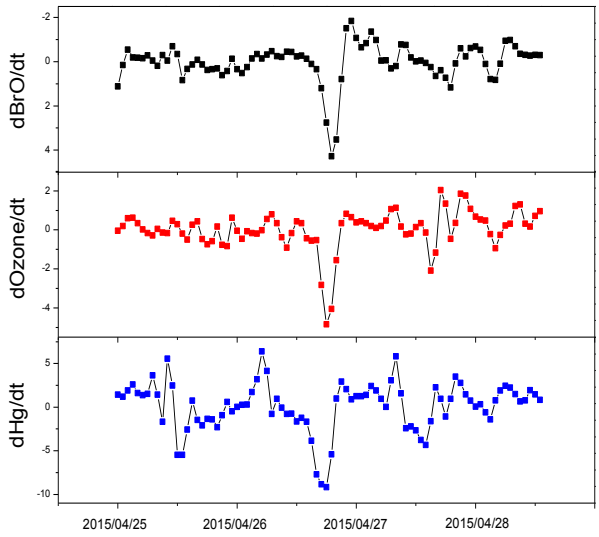

Fig. 13 –Time series of dBrO/dt, dO3/dt and dHg/dt during the BrO enhancement event